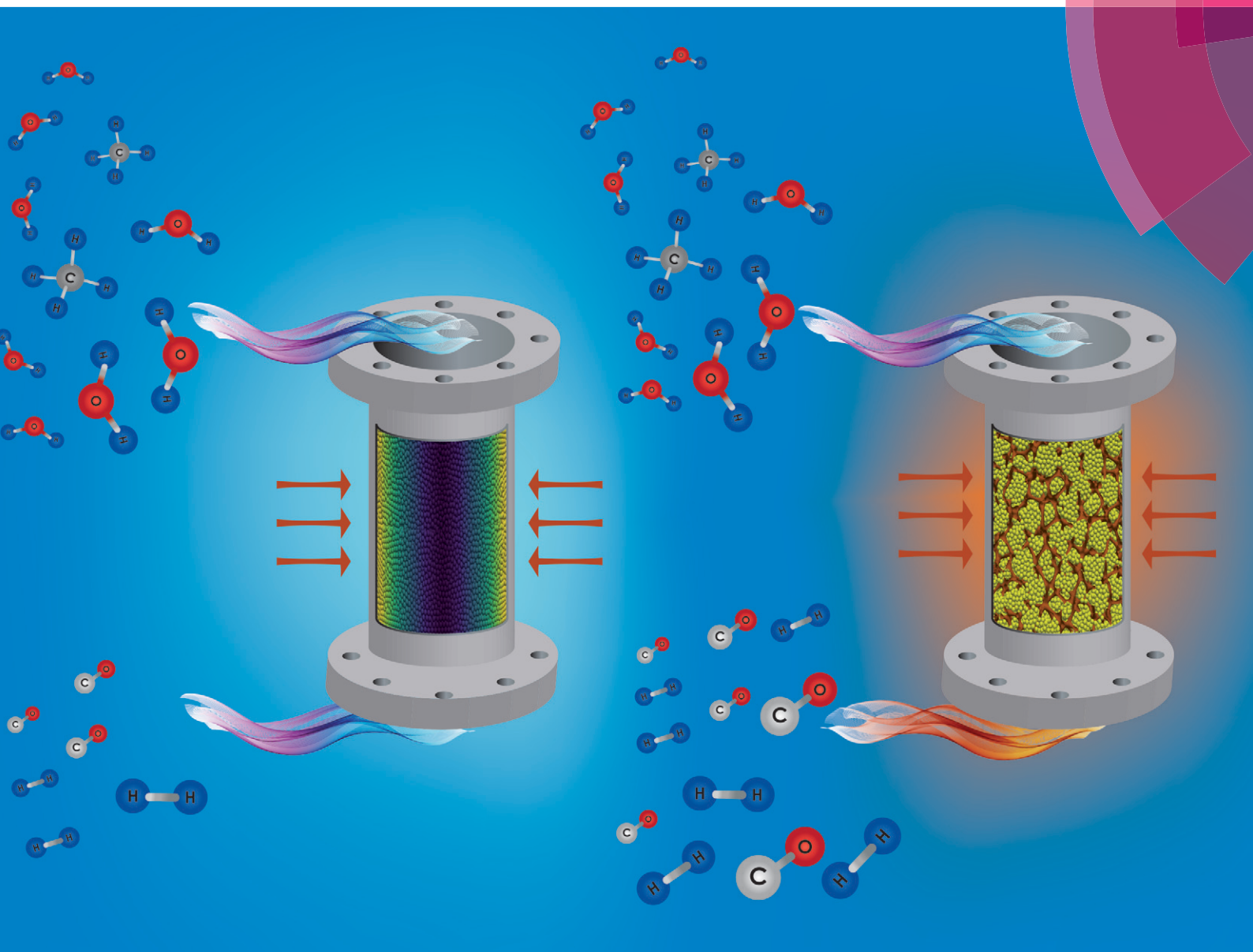


# Reaction Chemistry & Engineering

Linking fundamental chemistry and engineering to create scalable, efficient processes

[rsc.li/reaction-engineering](http://rsc.li/reaction-engineering)



ISSN 2058-9883



ROYAL SOCIETY  
OF CHEMISTRY

Celebrating  
IYPT 2019

## COMMUNICATION

Enrico Tronconi *et al.*

A comparison between washcoated and packed copper foams for the intensification of methane steam reforming





Cite this: *React. Chem. Eng.*, 2019, **4**, 1387

Received 20th March 2019,  
Accepted 2nd May 2019

DOI: 10.1039/c9re00125e

[rsc.li/reaction-engineering](http://rsc.li/reaction-engineering)

## A comparison between washcoated and packed copper foams for the intensification of methane steam reforming

Riccardo Balzarotti,  Alessandra Beretta,   
Gianpiero Groppi  and Enrico Tronconi \*

Different solutions for the intensification of the methane steam reforming process are proposed and tested. The intensification strategy involved, on the one side, the use of a highly active Rh/Al<sub>2</sub>O<sub>3</sub> catalyst and, on the other side, the development of advanced fixed bed reactor configurations wherein either washcoated or packed 40 PPI copper foams were used as highly conductive internals to improve heat transfer across the catalytic bed.

### 1. Introduction

Distributed hydrogen for the hydrogen economy calls for a profound change in the production and supply chain, such that it can respond to the need for compactness, energy efficiency, safety, flexibility and fast dynamic response to load changes that are typically associated with the operation of fuel cells, H<sub>2</sub>-fuelling stations or small scale industrial applications (e.g. metallurgy).<sup>1</sup> Due to its cost effectiveness, steam reforming of natural gas is currently the most used process to produce syngas and hydrogen.<sup>2</sup> This highly endothermic catalytic reaction is typically run in multitubular packed bed reactors, whose operation is limited by heat supply via a convective heat transfer mechanism, which relies on high flow rates; steam reformers are thus optimized for large-scale production.<sup>3</sup> In recent years, the intensification of fuel processors through the application of small scale and modular reformers has received considerable attention as a promising approach to achieve a distributed production system.<sup>4</sup> Such small-scale reformers require improved heat transfer performance, compact dimensions and lower flow rates in comparison with conventional full-scale reformers, which make the need for intensification of the limiting heat transfer performance of multi-tubular packed bed reactors even more urgent.

In order to overcome these limitations, the adoption of structured reactors has been proposed.<sup>5,6</sup> Among others, FeCrAl has been investigated as the material of choice to produce microchannel reactors, where steam reforming is coupled with exothermic reactions in a complex multi-flow system.<sup>6–8</sup> Additionally, the use of noble-metal-based catalysts (washcoats) has been proven to provide higher specific activity, smaller sizes, faster dynamic response, and higher thermal and start/stop stability than conventional Ni-based catalysts.<sup>6</sup>

Another approach to process intensification focuses on the improvement of the overall heat transfer properties of fixed bed reactors by introducing highly conductive metal substrates.<sup>5</sup> In this view, many studies are focused on the reforming of methanol, which is less energy intensive than the methane reforming process. Zhou *et al.* tested Cu/Zn/Al/Zr catalysts washcoated onto metal (e.g. nickel and copper) foams for methanol reforming in a microreactor, and better performance was found for the copper-supported samples over the Ni-based foam due to the high thermal conductivity of copper.<sup>9</sup> Shen *et al.* tested copper open cell foams as supports for rare earth metal-promoted Cu-based catalysts for methanol steam reforming in a compact microchannel reactor; in their conclusions, the authors claimed the minimization of cold spots with the use of the washcoated copper foam over the packed bed configuration.<sup>10</sup> Catillon *et al.* tested the combination of copper foams with a commercial Cu–ZnO/Al<sub>2</sub>O<sub>3</sub> catalyst to improve the heat exchange in a reactor, obtaining improvements with respect to a commercial catalyst in the form of pellets.<sup>11</sup>

Fewer efforts have been made to investigate the use of copper matrices in the highly energy demanding methane reforming process. Qi *et al.* investigated the deposition and catalytic activity of a Ni-based catalyst supported on Mg/Al metal oxide, which was washcoated onto a copper foam for solar dry reforming of methane.<sup>12</sup> Jang *et al.* studied the production of syngas and hydrogen by coupling methane reforming and water splitting under simulated solar-light

Politecnico di Milano, Dipartimento di Energia, Via La Masa 34, 20156 Milano, Italy. E-mail: [enrico.tronconi@polimi.it](mailto:enrico.tronconi@polimi.it)



irradiation, using different foam devices coated with  $\text{CeO}_2/\text{ZrO}_2$  layers.<sup>13</sup>

Previous studies of our research group documented the potential of metal foams to act as effective catalyst carriers thanks to the enhancement of heat transfer, which resulted from the presence of the solid, continuous and conductive metal matrix.<sup>14</sup> Recently a new reactor layout was proposed to overcome the intrinsic limitations associated with washcoated structured supports (*i.e.* washcoat adhesion, catalyst loading, and regeneration).<sup>15</sup> The approach consists of filling the empty pores of open-cell foams with small catalytic particles, thus pursuing the twofold goal of enhancing the radial and axial heat transfer processes, thanks to the presence of highly conductive and interconnected matrices, and having a high catalyst inventory. Despite the great potential of this reactor configuration, at the present time, the use of packed foams is at an early stage, with only one reported experimental application to a highly exothermic process, *i.e.* the Fischer–Tropsch synthesis.<sup>16</sup> The introduction of a highly conductive aluminum matrix made the operation of the reactor possible under much more severe conditions than those of a packed bed configuration, preventing the occurrence of thermal runaway even at 67% CO conversion.

Based on this background, the present work aims at implementing and testing two different reactor configurations based on the use of copper foams as solutions for intensifying the methane steam reforming process, namely a washcoated foam and a packed foam. In the first case, a thin catalytic layer was deposited by spin-coating onto the support surface, while in the second case, the support pores were filled with catalytic particles in the form of egg-shell spheres with a diameter of 600  $\mu\text{m}$ . A traditional packed bed loaded with the same amount of catalyst was tested as a reference.

Concerning the catalyst formulation, the intensification strategy also included the adoption of a highly active Rh/ $\text{Al}_2\text{O}_3$  catalyst. As widely established in the literature and recently reviewed by Farrauto,<sup>17</sup> noble metals allow the significant enhancement of the kinetics of methane steam reforming, thus meeting the need for a smaller catalyst inventory. Among precious metals, Rh is widely recognized as the best-performing active element with a reduced tendency toward coking phenomena. In our laboratory, know-how was gained through years of preparing, washcoating and analyzing the kinetics of Rh/ $\text{Al}_2\text{O}_3$  catalysts for syngas production processes from methane and light hydrocarbons;<sup>18</sup> this provided a background for the proposal of an active, selective and stable catalyst for the development of innovative structured reactors based on the use of Cu foams.

## 2. Experimental

### 2.1. Catalyst preparation and characterization

An egg-shell catalyst was prepared by dry-impregnation of a rhodium nitrate solution ( $\text{Rh}(\text{NO}_3)_3$  liquid solution, 12.5% wt metal content by Alfa Aesar) on alumina particles with a nominal diameter of 600  $\mu\text{m}$  (PURALOX by Sasol) according

to a procedure reported in the literature.<sup>19</sup> The catalyst was prepared while aiming for a final Rh metal content of 0.3% wt with respect to the alumina carrier mass and for an egg-shell thickness of 35  $\mu\text{m}$ , which corresponds to 1% wt of metallic Rh with respect to the alumina eggshell mass.

The powder catalyst was prepared by incipient wetness impregnation using a rhodium nitrate solution ( $\text{Rh}(\text{NO}_3)_3$  liquid solution, 12.5% wt metal content by Alfa Aesar) to activate  $\gamma\text{-Al}_2\text{O}_3$  powder (SCFa-140 by Sasol) aiming for the same metallic active phase content per unit mass as the one found in the eggshell layer (*i.e.* 1% wt of metallic Rh with respect to the  $\gamma\text{-Al}_2\text{O}_3$  powder mass). Before impregnation, the  $\gamma\text{-Al}_2\text{O}_3$  powder was calcined at 800  $^\circ\text{C}$  for 10 h at heating and cooling rates of 2  $^\circ\text{C min}^{-1}$ .

In order to have the same amount of metal active phase per unit volume of the reactor and according to the morphological properties of the copper foam, an average washcoat load of 10.5% wt with respect to the mass of the copper foam was deposited; the latter corresponds to an average washcoat layer thickness of 80  $\mu\text{m}$ .

The washcoated foam (WF) was prepared by the slurry coating technique using a formulation reported in the literature.<sup>20</sup> Based on previous work,<sup>21</sup> spin coating was the deposition technique of choice to properly tune the washcoat layer mass and to prevent foam pore clogging. The spin coating speed and time were set to 1500 rpm and 10 s, respectively, using a lab-scale spin coater device (Spin150i model by SPS).

Both the powder catalyst and the egg-shell particles have been characterized to assess the chemical and physical properties of the materials. In particular, ICP-MS measurements (XSeries II by Thermo Fisher) were carried out to determine the final Rh content. Based on procedures reported in the literature,<sup>22</sup> the active metal phase and dispersion were further characterized by TPD-R and chemisorption tests using a TPD/R/O 1100 catalytic surface analyzer (Thermo Electron). For both powder and egg-shell catalysts, metal dispersion was found to be in the 90% range.

The alumina support surface area was evaluated by means of BET measurements (TriStar 3000 device by Micromeritics); surface areas of 160 and 140  $\text{m}^2 \text{g}^{-1}$  were found for the  $\text{Al}_2\text{O}_3$  particles and  $\text{Al}_2\text{O}_3$  powder, respectively. The rheological behavior of the slurry was characterized by using a rotational rheometer with a disc-plate configuration (DSR 200 device by Rheometrics); viscosity was evaluated in the shear rate range of 1–1000  $\text{s}^{-1}$ .

### 2.2. Catalytic tests

All the catalytic tests on the structured reactors were performed using the same internal, namely a 40 PPI (pores per inch) copper foam ( $\varepsilon = 0.88$ ,  $S_v = 1220 \text{ m}^{-1}$  and cell size = 2 mm) by Duocel. The foam diameter and height were set to 29 mm and 25 mm, respectively. In the packed bed (PB) and packed foam (PF) configurations, a dilution factor was used to obtain the same weight of catalyst per unit volume as in the packed foam. In particular, dilutions of 1.54 and 0.51





were used for the PB and PF systems, respectively (values refer to the weight ratio between the dilutant mass and catalyst mass). Inert alumina particles were used for the PF system, while silicon carbide particles were used for the PB system.

The catalytic tests were performed in a tubular stainless steel reactor with a length and internal diameter equal to 400 and 29.5 mm, respectively. A premixed bed of silicon carbide particles was placed on top of the catalytic bed; an inert 40 PPI FeCrAl empty open cell foam was placed below the catalytic bed as a space holder.

Temperature profiles were recorded longitudinally across the catalytic beds using three K-type thermocouples with an external diameter of 1 mm, sliding inside stainless steel-wells with an outer diameter of 1/8". The thermocouples were placed at three different radial positions, namely at the centerline (center-T in the following), at 8 mm from the center in a radial position (radial-T) and outside the reactor wall (wall-T). Catalytic tests were performed at two different space velocities, namely 5000 and 10000 h<sup>-1</sup>. The reactor was heated externally using a furnace (RT 50-250/11 model by Nabertherm) and catalytic tests were performed by setting the furnace temperature in the 700–800 °C range, with a step of 50 °C, at atmospheric pressure.

A steam/CH<sub>4</sub> mixture was fed to the reactor; the steam-to-carbon ratio (S/C) was set to 3.5 and water was fed in the liquid form; evaporation and reactant mixing took place in the premixed silicon carbide bed that was placed on the top of the catalytic bed. Unreacted water was condensed downstream from the reactor and the composition of gaseous reaction products was measured using an on-line micro-GC (GCX model by Pollution) equipped with MolSieve and Porapak columns connected to TCD detectors. The CO concentration was determined by carbon balance over gas chromatography analysis; the overall absolute errors detected in carbon balances were in the range of 1–5%.

## 3. Results and discussion

### 3.1. Catalyst characterization

The preliminary characterization carried out on the catalytic slurry by rheological measurements showed a slightly non-Newtonian rheological behavior, with the viscosity decreasing from 0.12 Pa s<sup>-1</sup> at a shear rate of 1 s<sup>-1</sup> to 0.07 Pa s<sup>-1</sup> at 1000 s<sup>-1</sup>. This is in accordance with results reported in the literature for other catalytic slurries based on the same dispersing medium.<sup>20</sup>

The washcoating process consisted of a sequence of deposition and flash drying steps, with intermediate monitoring of the washcoat load evolution until reaching the final desired load. The final washcoat load of 10.5% wt was obtained after 6 consecutive depositions; notably, a linear growth of the washcoated layer onto the foam surface of about 1.8% wt per deposition was measured, which was a preliminary indication of the absence of pore clogging phenomena. Additionally, good reproducibility of the whole procedure was obtained, based on the production of replicated samples. The

promising results obtained by gravimetric analysis are confirmed by optical microscopy analysis, whose results are reported in Fig. 1.

The results obtained by optical microscopy also demonstrated a good and homogeneous coverage of the foam surface, without any relevant occurrence of pore clogging phenomena. This is probably due to the high shear stresses induced on the slurry during the spin coating process.<sup>21</sup>

Fig. 2 shows the cross-sectional image of an egg-shell particle. An average shell thickness of 32 ± 4 μm was found after reduction in the TPD/R tests.

### 3.2. Catalytic tests

The methane steam reforming experiments were performed in three configurations under conditions of interest for the real application; in each test, reactor performances were characterized in terms of axial and radial temperature distributions, as well as in terms of methane conversion.

Fig. 3 shows the temperature profiles for the packed foam (PF, c) and washcoated foam (WF, b) samples measured at 10000 h<sup>-1</sup> and at an oven temperature of 800 °C. The profiles for the packed bed system (PB, a) are reported as the benchmark of a conventional steam reforming system.

The introduction of the conductive copper matrix caused remarkable changes in the temperature distribution across the beds. The maximum radial temperature difference between the reactor wall and centerline was found to decrease from 132 °C (PB) to 50 °C and 47 °C for the WF and PF

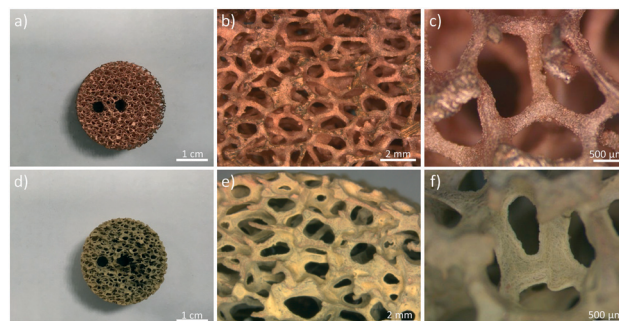


Fig. 1 Optical microscopy images of the bare foam (a–c) and of the washcoated sample after flash drying (d–f) at different magnifications.

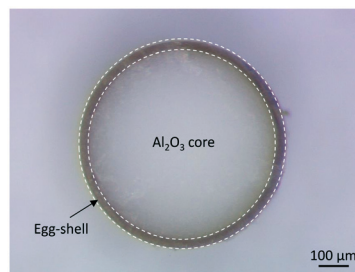


Fig. 2 Optical microscopy image of the cross section of an egg-shell catalytic particle after the reduction process.



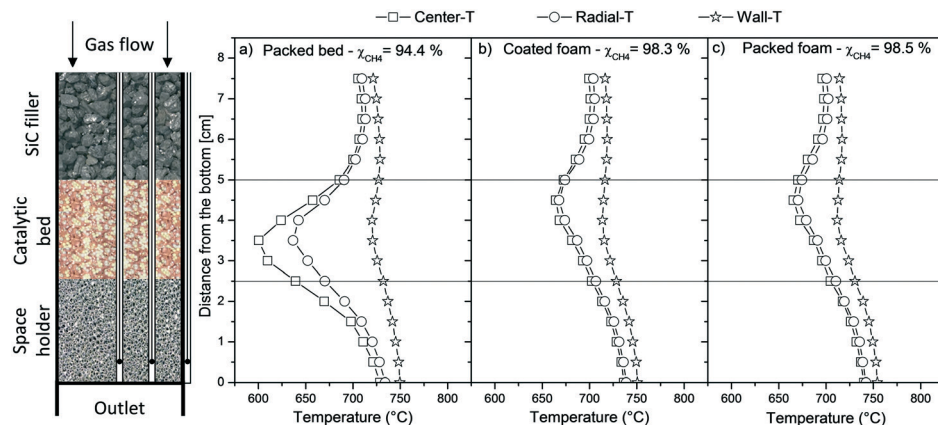


Fig. 3 Axial temperature profiles measured at the three radial positions (*i.e.* reactor centerline (square), half radius (circle) and external reactor wall (star)) for the packed bed (a), washcoated foam (b) and packed foam (c) configurations.  $T_{\text{oven}} = 800\text{ }^{\circ}\text{C}$  and GHSV =  $10\,000\text{ h}^{-1}$ .

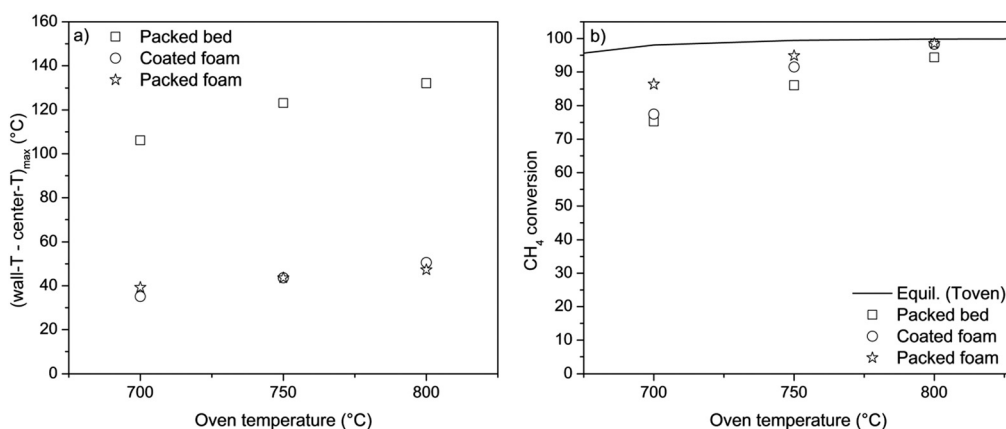


Fig. 4 Maximum radial temperature difference as a function of oven temperature (a) and methane conversion as a function of oven temperature (b) for the packed bed, washcoated foam and packed foam configurations. GHSV is set to  $10\,000\text{ h}^{-1}$ .

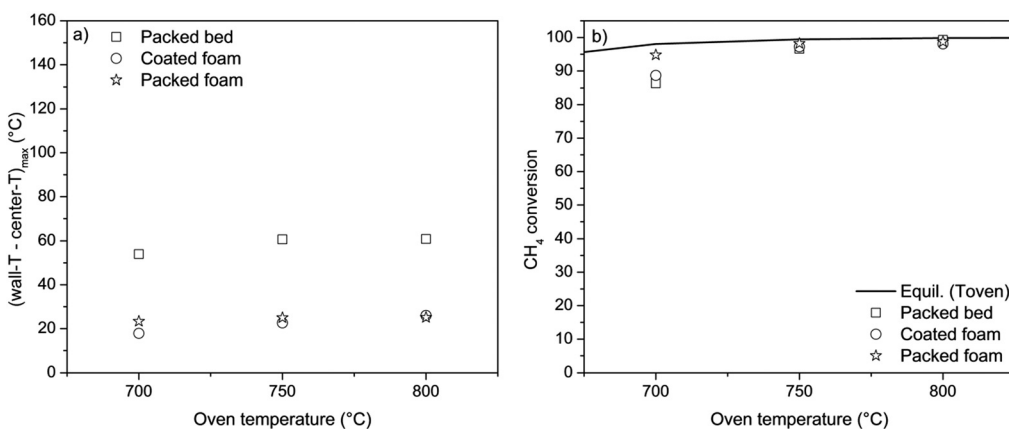


Fig. 5 Maximum radial temperature difference *versus* oven temperature (a) and methane conversion *versus* oven temperature (b) for the packed bed, washcoated foam and packed foam configurations. GHSV is set to  $5\,000\text{ h}^{-1}$ .

samples, respectively. Besides, the entire central and radial temperature profiles changed in the presence of the Cu-internals; in fact, they were found to be nearly overlapped in the PF and WF configurations, in contrast with the results found for the PB system. This is clear evidence of the en-

hanced heat transfer in the radial direction induced by the presence of the highly conductive copper matrix, which enabled smaller radial temperature gradients across the whole bed length. In particular, the presence of the solid conductive copper matrix enhanced the overall performance by reducing



the heat transfer resistance from the reactor wall to the catalytic bed, compared with the packed bed operated at the very low gas velocity characteristic of the present study. In addition to the milder temperature gradients, an improvement in the methane conversion was found as it increased from 94% (PB system) to 98% (WF and PF systems). Although small, this improvement is significant given the fundamental role of thermodynamics at these high temperatures, and it is likely due to the more uniform temperature distribution enabled by the conductive foam.

Similar results were observed by changing the process temperature, as reported in Fig. 4, where the maximum radial temperature difference and the conversion are plotted against the furnace temperature setting.

The temperature measurements (Fig. 4a) confirmed the dominant role of the high conductivity of the solid matrix under these reaction conditions. Moreover, despite the clear differences between the WF and PF reactor layouts, there is apparently no difference from the point of view of temperature gradients; in fact, at any oven temperature, very close values of the maximum temperature difference (*i.e.* (wall-T – center-T)<sub>max</sub> reported in Fig. 4a) were measured in the WF and PF. This indicates that the radiative contribution, which is expected due to the WF open structure,<sup>23</sup> did not provide any significant advantage even at 800 °C, being likely compensated by the improvement of the wall heat transfer coefficient associated with the packed particles in PF.<sup>15</sup> Additional experimental investigations and a dedicated modelling analysis are needed to fully elucidate and quantify the contributions of the different heat transfer mechanisms, which will address the interactions among the copper matrix, the gas-packed bed pseudo-phase and/or the washcoat. This analysis will require a specific kinetics study to match the global heat transfer mechanisms with the local heat consumption contributions associated with the heterogeneous chemical process.<sup>24</sup>

At this stage of the work, it is of great interest to notice that the strongly enhanced heat transfer properties of the copper-based layouts determined an improvement in the integral methane conversion over the packed bed system, as evidenced in Fig. 4b. This result is especially remarkable, given the approach to thermodynamic equilibrium under our experimental conditions. Further kinetic investigations will also clarify the possible differences in the catalytic activity of copper-based configurations.

Tests at 5000 h<sup>-1</sup> showed, at all temperatures, similar trends in terms of both temperature gradients (Fig. 5a) and methane conversions (Fig. 5b).

## Conclusions

This communication reports for the first time the successful application of Cu cellular matrices to the intensification of methane steam reforming. Both a washcoated foam and the novel concept of foam packed with catalyst particles have been tested and compared with a conventional packed bed

configuration. Based on the experimental results reported in this paper, the following conclusions can be drawn.

Copper is a suitable material for running the reforming process at temperatures as high as 800 °C. The copper foam can be used advantageously both as a geometrical conductive substrate for a washcoated catalyst (WF configuration) or as a conductive internal to enhance heat transfer in the radial direction (PF configuration). The latter configuration is entirely new; the application of packed foams to methane steam reforming has not been reported previously to our knowledge. At the low gas velocities investigated here, an evident reduction of the radial temperature gradients and, consequently, a significant improvement in the methane conversion are provided by the copper-based WF or PF configurations, in comparison with the conventional PB system.

The results herein presented concerning the use of copper matrices should be regarded as preliminary; detailed ongoing studies of the influence of the foam properties on the overall system performance may lead to further intensification of the process.

## Conflicts of interest

There are no conflicts to declare.

## Acknowledgements

The research leading to these results has received funding from the European Research Council under the European Union's Horizon 2020 Research and Innovation Program (Grant Agreement no. 694910/INTENT).

## Notes and references

- 1 S. Specchia, *Int. J. Hydrogen Energy*, 2014, **39**, 17953–17968.
- 2 L. Baharudin and M. J. Watson, *Rev. Chem. Eng.*, 2017, **34**, 43–72.
- 3 O. Sanz, I. Velasco, I. Reyero, I. Legorburu and G. Arzamendi, *Catal. Today*, 2016, **273**, 131–139.
- 4 G. Kolb, *Chem. Eng. Process.*, 2013, **65**, 1–44.
- 5 L. Baharudin and M. J. Watson, *Rev. Chem. Eng.*, 2018, **34**, 481–501.
- 6 R. J. Farrauto, Y. Liu, W. Ruettinger, O. Ilinich, L. Shore and T. Giroux, *Catal. Rev.: Sci. Eng.*, 2007, **49**, 141–196.
- 7 G. Kolb, V. Hessel, V. Cominos, H. Pennemann, J. Schürer, R. Zapf and H. Löwe, *J. Mater. Eng. Perform.*, 2006, **15**, 389–393.
- 8 A. K. Avcı, D. L. Trimm and M. Karakaya, *Catal. Today*, 2010, **155**, 66–74.
- 9 W. Zhou, Y. Ke, Q. Wang, S. Wan, J. Lin, J. Zhang and K. S. Hui, *Fuel*, 2017, **191**, 46–53.
- 10 C. C. Shen, T. Y. Jian and Y. T. Wang, *Fuel Cells*, 2013, **13**, 965–970.
- 11 S. Catillon, C. Louis and R. Rouget, *Top. Catal.*, 2004, **30**, 463–467.



- 12 J. Qi, Y. Sun, Z. Xie, M. Collins, H. Du and T. Xiong, *J. Energy Chem.*, 2015, **24**, 786–793.
- 13 J. T. Jang, K. J. Yoon and G. Y. Han, *Sol. Energy*, 2014, **101**, 29–39.
- 14 P. Aghaei, C. G. Visconti, G. Groppi and E. Tronconi, *Chem. Eng. J.*, 2017, **321**, 432–446.
- 15 C. G. Visconti, G. Groppi and E. Tronconi, *Catal. Today*, 2015, **273**, 178–186.
- 16 L. Fratalocchi, C. G. Visconti, G. Groppi, L. Lietti and E. Tronconi, *Chem. Eng. J.*, 2018, **349**, 829–837.
- 17 R. J. Farrauto, *Chem. Eng. J.*, 2014, **238**, 172–177.
- 18 A. Beretta, A. Donazzi, G. Groppi, M. Maestri, E. Tronconi and P. Forzatti, in *Catalysis: Volume 25*, The Royal Society of Chemistry, 2013, vol. 25, pp. 1–49.
- 19 A. Porta, L. Falbo, C. G. Visconti, L. Lietti, C. Bassano and P. Deiana, *Catal. Today*, DOI: 10.1016/J.CATTOD.2019.01.042, in press.
- 20 R. Balzarotti, C. Cristiani, S. Latorrata and A. Migliavacca, *Part. Sci. Technol.*, 2016, **34**, 184–193.
- 21 R. Balzarotti, C. Cristiani and L. F. Francis, *Surf. Coat. Technol.*, 2017, **330**, 1–9.
- 22 A. Beretta, A. Donazzi, G. Groppi, P. Forzatti, V. Dal Santo, L. Sordelli, V. De Grandi and R. Psaro, *Appl. Catal., B*, 2008, **83**, 96–109.
- 23 C. Y. Zhao, T. J. Lu and H. P. Hodson, *Int. J. Heat Mass Transfer*, 2004, **47**, 2927–2939.
- 24 A. Donazzi, A. Beretta, G. Groppi and P. Forzatti, *J. Catal.*, 2008, **255**, 241–258.

